Conf-8206160--1

CONF-8206160--1

DE83 007617

IMPURITY DIFFUSION IN TRANSITION-METAL OXIDES*

N. L. PETERSON

Materials Science Division
Argonne National Laboratory, Argonne, IL 60439

The submitted manuscript has been authored by a contractor of the U. S. Government under contract No. W-31-109-ENG-38. Accordingly, the U. S. Government retains a nonexclusive, royalty-free license to publish or reproduce the published form of this contribution, or allow others to do so, for U. S. Government purposes.

JUNE 1982

DISCLAIMER

This report was prepared as an account of work sponsored by an agency of the United States Government. Neither the United States Government nor any agency thereof, nor any of their employees, makes any warranty, express or implied, or assumes any legal liability or responsibility for the accuracy, completeness, or usefulness of any information, apparatus, product, or process disclosed, or represents that its use would not infringe privately owned rights. Reference herein to any specific commercial product, process, or service by trade name, trademark, manufacturer, or otherwise does not necessarily constitute or imply its endorsement, recommendation, or favoring by the United States Government or any agency thereof. The views and opinions of authors expressed herein do not necessarily state or reflect those of the United States Government or any agency thereof.

MASTER

*Work supported by the U.S. Department of Energy.

To be published in Solid State Ionics

DISTRIBUTION OF THIS DOCUMENT IS UNLIMITED

IMPURITY DIFFUSION IN TRANSITION METAL OXIDES*

N. L. PETERSON

Materials Science Division
Argonne National Laboratory, Argonne, IL 60439

ABSTRACT

Intrinsic tracer impurity diffusion measurements in ceramic oxides have been primarily confined to CoO, NiO, and Fe_3O_4. Tracer impurity diffusion in these materials and TiO_2, together with measurements of the effect of impurities on tracer diffusion (Co in NiO and Cr in CoO), are reviewed and discussed in terms of impurity-defect interactions and mechanisms of diffusion. Divalent impurities in divalent solvents seem to have a weak interaction with vacancies whereas trivalent impurities in divalent solvents strongly influence the vacancy concentrations and significantly reduce solvent jump frequencies near a trivalent impurity. Impurities with small ionic radii diffuse more slowly with a larger activation energy than impurities with larger ionic radii for all systems considered in this review. Cobalt ions (a moderate size impurity) diffuse rapidly along the open channels parallel to the c-axis in TiO_2 whereas chromium ions (a smaller-sized impurity) do not.

IMPURITY DIFFUSION IN TRANSITION METAL OXIDES*

N. L. PETERSON

Materials Science Division
Argonne National Laboratory, Argonne, IL 60439

1. Introduction

Impurity diffusion is the transport of any species other than the host material in the solid. Two types of impurity diffusion coefficients are commonly used in the literature. The interdiffusion coefficient $\tilde{D}$ describes the process by which two adjacent solids of differing compositions homogenize by the mutual diffusion of species across a common boundary. This coefficient is composition dependent (hence, a function of position within the sample), and its interpretation in terms of defect properties is complicated by the presence of compositional gradients and net mass flow. The tracer diffusion coefficient D* refers to either self- or impurity diffusion when the species of interest is at infinitely small concentration. The tracer diffusion coefficient is independent of position in a homogeneous sample; even though there is a gradient of the radioactivity as a function of distance, a given atom "sees" only a homogeneous solid. Owing to the greater accuracy of measurement and ease of interpretation, only tracer diffusion experiments will be considered in this paper.

---

*Work supported by the U.S. Department of Energy.

Two types of tracer-impurity diffusion measurements may be made that complement each other and help identify the details of the impurity diffusion process.

(a) The motion of an isolated impurity ion in an otherwise pure crystal may be measured. The availability of high specific activity (often carrier-free) tracers allow measurements to be made at indiffused-impurity concentrations below the intrinsic defect concentration. Under these conditions the tracer atom follows a jump sequence as though no other impurity ions were in the crystal and at a defect concentration corresponding to the pure crystal. The diffusion process is then relatively simple to treat theoretically. It is necessary only to specify the atomic jump frequencies and defect interaction energies for the few simple and well-defined solute-defect configurations. Impurity diffusion under these conditions in NiO, $Co_{1-\delta}O$, Fe_3O_4, and TiO_2 will be reviewed in sections 2 to 4.

(b) Self- and impurity tracer diffusion may be measured in crystals doped with controlled amounts of the impurity. The dopant will influence the concentration of defects and jump frequencies of the ions throughout the crystal, but the concentration of an indiffused tracer is sufficiently low that D* will be independent of position in the sample. If the concentration of randomly spaced impurity ions is sufficiently low so that the spheres of influence of different impurity atoms do not overlap (1-2% dopant), the theory may be sufficiently simple to allow details of the impurity diffusion process to be deduced. The effect of Co additions to

NiO and Cr addition to $Co_{1-\delta}O$ on tracer diffusion will be discussed in section 5.

2. Impurity Diffusion in NiO and $Co_{1-\delta}O$

Before the results for impurity diffusion in NiO and $Co_{1-\delta}O$ are considered, the general formalism for impurity diffusion will be briefly discussed.

2.1 Impurity diffusion formalism

The temperature dependence of the tracer self-diffusion coefficient is frequently found to obey the Arrhenius equation

$$D^s = D_o^s \exp(- Q^s/kT). \tag{1}$$

From simple reaction-rate theory, one may obtain the expressions

$$Q^s = h_f^s + h_m^s \tag{2}$$

and

$$D_o^s = a^2 \nu^s f^s \exp[(s_f^s + s_m^s)/k] \tag{3}$$

for diffusion by a simple-defect mechanism in a cubic structure. The superscript s refers to self-diffusion; h_f and h_m are the enthalpies and s_f and s_m are the enthropies of defect formation and migration, respectively; a is the edge length of the elementary cube; ν is the vibration frequency of an atom about its equilibrium position in the jump direction; and f is

the correlation factor that accounts for the non-randomness of tracer atom jumps. For self-diffusion, f^s is generally a temperature-independent constant that is determined by the diffusion mechanism and the crystal symmetry [1].

For impurity diffusion, the correlation factor f^i depends on the relative jump frequencies of the impurity and the neighboring solvent ions. The presence of the impurity will change the values of the jump frequencies of the neighboring solvent atoms relative to the values in the absence of the impurity. Assuming that the effect of the impurity is short-ranged, four different jump frequencies for the vacancy near an impurity ion may be defined for the fcc lattice. As shown in fig. 1, w_1 is the frequency of exchange of a vacancy neighboring an impurity ion with any of the four solvent ions that are also neighbors of the impurity; w_2 is the frequency of exchange of the impurity and the vacancy; w_3 is the frequency of exchange of a vacancy neighboring an impurity with any of the seven solvent ions adjacent to the vacancy but not neighbors of the vacancy (dissociation jumps); w_4 is the frequency of the association jump (reverse of a w_3 jump); and all other jumps are assumed to take place with a frequency w_o, which is the frequency of the solvent-vacancy exchange in the pure solvent. The correlation factor for impurity diffusion f^i in the fcc lattice may be expressed in terms of these various jump frequencies;

$$f^i = \frac{w_1 + 7/2\ Fw_3}{w_1 + w_2 + 7/2\ Fw_3}, \qquad (4)$$

where F is the fraction of vacancies making w_3 jumps that effectively do not return to the site from which the w_3 jump was made; F is a known function of w_4/w_o [2].

If there is an impurity-vacancy interaction, the energy to form a vacancy next to an impurity h_f^i will be different from h_f^s. Similarly, the energy for an impurity-vacancy exchange h_m^i may be different from h_m^s. The activation energy for impurity diffusion Q^i will differ from Q^s by an amount

$$\Delta Q = Q^i - Q^s = (h_m^i - h_m^s) + (h_f^i - h_f^s) - C$$

$$= \Delta h_m + \Delta h_f - C, \tag{5}$$

where $-\Delta h_f$ is the impurity-vacancy binding energy h_b^{i-v} and C is the temperature dependence of f^i;

$$C = R \frac{\partial \ln f^i}{\partial (1/T)} . \tag{6}$$

Each of the w_j's in eq. (4) may be written in the form of an Arrhenius equation:

$$w_j = \nu_j \exp(s_m/k) \exp(- h_{m,j}/kT). \tag{7}$$

Since the various $h_{m,j}$'s may be different, f^i will vary with temperature. Values of Δh_m, Δh_f, and C have been calculated for a large number of impurities diffusing in Cu, Ag, Al, and Cd [3]; good agreement between theory and experiment is found when a realistic interatomic potential is available. Similar calculations have not been reported for metal oxides;

however, the formalism above is valid for oxides and is useful for discussing experimental results.

2.2 Defect structure and mobility in NiO and $Co_{1-\delta}O$

The oxides NiO and $Co_{1-\delta}O$ (also $Mn_{1-\delta}O$ and $Fe_{1-\delta}O$) have the NaCl structure and are metal-deficient at high temperatures [4]. The oxides can be described by a general formula, $M_{1-\delta}O$, in which the non-stoichiometric defect has been generally recognized as a cation vacancy. Electroneutrality in the crystal is preserved by the presence of an appropriate number of electron holes that compensate for missing cations. The value of δ is less than 10^{-3} for NiO and less than 10^{-2} for $Co_{1-\delta}O$. The defect structure and mobility is better known for $Co_{1-\delta}O$. The details of this defect structure that influence impurity diffusion are discussed in the following paragraphs for $Co_{1-\delta}O$.

The extensive measurements of the deviations from stoichiometry δ as a function of p_{O_2} [5-10] show an excess of oxygen ions relative to cobalt ions in $Co_{1-\delta}O$. The rapid cation tracer diffusion [5, 11-14] relative to anion tracer diffusion [15] ($D^*_{Co}/D^*_O \sim 5\times10^4$ at 1200°C) strongly suggests that the excess oxygen ions are accommodated by the formation of cation vacancies (and electron holes) rather than anion interstitials. Various charges are possible for the cation vacancies. The formation of neutral vacancies can be expressed as follows:

$$\tfrac{1}{2}O_2(g) = V^x_{Co} + O^x_O \,. \qquad (8)$$

Singly charged vacancies can be formed by the dissociation of neutral vacancies:

$$V^{x} = V'_{Co} + \dot{h} \; . \tag{9}$$

Further dissociation of electron holes yields doubly charged vacancies:

$$V'_{Co} = V''_{Co} + \dot{h} \; . \tag{10}$$

If only one type of cation vacancy is present, and the defect concentration is sufficiently small that defect-defect interactions can be neglected, then the application of the law of mass action to eqs. (8-10) allows one to relate the defect concentration to the oxygen partial pressure:

$$[V^{x}_{Co}] \propto (p_{O_2})^{1/2} \tag{11}$$

$$[V'_{Co}] \propto (p_{O_2})^{1/4} \tag{12}$$

$$[V''_{Co}] \propto (p_{O_2})^{1/6} . \tag{13}$$

The simplified electroneutrality condition

$$[\dot{h}] = [V'_{Co}] + 2\,[V''_{Co}] \tag{14}$$

was used in the derivation of eqs. (11-13). The deviation from stoichiometry is given by the relation

$$\delta = [V^{x}_{Co}] + [V'_{Co}] + [V''_{Co}] . \tag{15}$$

If the mean lifetime of the various charged cation vacancies is small

compared with the mean time-of-stay between vacancy jumps (i.e., the hole mobility is much greater than the vacancy mobility), then only one jump frequency need be considered for all vacancies. If this jump frequency is independent of the defect concentration, then a measurement of the cation tracer diffusivity D^* as a function of p_{O_2} may be related to δ and provide a determination of the dominant vacancy type.

Several measurements of δ [7], electrical conductivity [6,9,16] and D^*_{Co} [13,14] cover a large range of p_{O_2}. These measurements show a curved plot vs p_{O_2}, indicating that more than one type of defect is present in $Co_{1-\delta}O$. The results of Dieckmann [13] for D^*_{Co} are shown in fig. 2. Dieckmann has made an extensive analysis of the literature data on the p_{O_2} dependence of δ, D^*_{Co}, and electrical conductivity. He concludes that the concentration of cobalt interstitials and oxygen vacancies are negligible; the dominant defects are vacancies on the cation sublattice and electron holes, and the vacancies can be formally treated as neutral, singly charged, or doubly charged. The appropriate equilibrium constants for the reactions given by eqs. (8-10) are as follows [13]:

$$K_8 = \frac{[V^x_{Co}]}{p^{1/2}_{O_2}} = 1.6\times10^{-2} \exp[-26{,}000\ (J/mol)/RT]; \tag{16}$$

$$K_9 = \frac{[V'_{Co}][\dot{h}]}{[V^x_{Co}]} = 2.4 \exp[-51{,}000\ (J/mol)/RT]; \tag{17}$$

$$K_{10} = \frac{[V''_{Co}][\dot{h}]}{[V'_{Co}]} = 0.17 \exp[-72{,}000\ (J/mol)/RT]. \tag{18}$$

The normalized D^*_{Co} and electrical conductivity may be described by [13]

$$D^*_{Co}/\Sigma[V_{Co}] = 0.113 \exp[-136{,}000\ (J/mol)/RT]\ (cm^2/s) \quad (19)$$

and

$$\sigma/[\dot{h}] = 5.4\times10^3 \exp[-8{,}600\ (J/mol)/RT]\ (\Omega\cdot cm)^{-1}, \quad (20)$$

thus justifying the earlier assumption that the hole mobility is much greater than the vacancy mobility.

The curvature in the plots of log D^*_{Co} vs log p_{O_2} shown in fig. 2 can be quantitatively interpreted in terms of a change in relative contributions of differently charged vacancies with varying p_{O_2}, as shown by Dieckmann [13]. Other possible interpretations of the data include (a) impurity-induced (extrinsic) defects at low p_{O_2} and (b) defect clustering at high p_{O_2}. Chen and Peterson [14] have measured the isotope effect for D^*_{Co} as a function of p_{O_2} and observed values of $f\Delta K$ that are independent of p_{O_2} and consistent with diffusion by noninteracting vacancies and $\Delta K = 0.75$. Only the change in relative contribution of differently charged vacancies with varying p_{O_2} is consistent with the p_{O_2}-independent value of $f\Delta K$. The other possible causes of curvature are expected to produce an observable p_{O_2}-dependent value of $f\Delta K$ within the accuracy of the experiment; impurity-induced defects, defect clustering, and Frenkel defects do not make a major contribution to cation self-diffusion in $Co_{1-\delta}O$ at 1200°C.

Equation (19) indicates that $D^*_{Co}/\Sigma[V_{Co}]$ is independent of p_{O_2} at a given temperature, i.e., either all vacancies, independent of charge, move with the same activation energy (h_m = 136 kJ/mol = 32.5 kcal/mol) or only one type of vacancy is mobile. It was previously mentioned that if the

lifetimes of the various charged cation vacancies is small as compared to the mean time of stay of a vacancy, the vacancy may change its charge state many thousands of times between jumps and only one activation energy corresponding to the energetically most favorable vacancy charge state is required to describe cation-vacancy exchange in $Co_{1-\delta}O$. The actual charge state of the vacancy during the jump is unknown. Without prior knowledge of the vacancy charge state during the jump process, potential gradient studies cannot be safely used to determine point defect concentrations or mobilities in a material like $Co_{1-\delta}O$ [13]; theoretical calculations of this charge state will also be necessary for reliable calculations of activation energies for impurity diffusion.

Most of the features of the defect chemistry of $Co_{1-\delta}O$ are also applicable to NiO and $Mn_{1-\delta}O$. The electrical-conductivity [17] and cation self-diffusion [18] measurements require both singly and doubly charged vacancies in NiO, and only one activation energy for defect migration (h_m = 150 kJ/mol = 36 kcal/mol) [17] seems appropriate. Self-diffusion and the isotope effect for cation migration in $Mn_{1-\delta}O$ are consistent with migration by neutral, singly, and doubly charged vacancies; defect-defect interactions do not influence the diffusion until δ is greater than 0.01 [19]. Also, only one activation energy for defect migration seems appropriate in $Mn_{1-\delta}O$.

2.3 Results for impurity diffusion in NiO and $Co_{1-\delta}O$.

In addition to cation self-diffusion [12,18,20-22], tracer diffusion has been measured in NiO for the following impurities; Co [12,22,23], Cr

[24], and Fe [12]. The results for impurity diffusion and self-diffusion (including anion self-diffusion [25]) in NiO at p_{O_2} = 0.21 atm are shown in the form of Arrhenius plots in fig. 3. The results for cation self-diffusion and Fe impurity diffusion have been adjusted to p_{O_2} = 0.21 atm from the p_{O_2} of measurement (p_{O_2} = 1 atm) using the relation $D \propto p_{O_2}^{1/6}$. Since the published results for ^{35}S diffusion in NiO [26-28] may represent diffusion along dislocations or subboundaries [29], they are not included in fig. 3.

Tracer diffusion has been measured in $Co_{1-\delta}O$ for Co [5,11-13,22], O [15], Cr [30], Fe [12], and Ni [12,22] ions. The results for impurity diffusion and self-diffusion in $Co_{1-\delta}O$ at p_{O_2} = 0.21 atm are shown in the form of Arrhenius plots in fig. 4. The results for Fe impurity diffusion have been adjusted to p_{O_2} = 0.21 atm from the p_{O_2} of measurement (p_{O_2} = 1 atm) using the relation $D \propto p_{O_2}^{1/4}$. The published results for ^{35}S diffusion in $Co_{1-\delta}O$ [28] are not included for the reasons given above for NiO.

The activation energies for cation tracer diffusion in NiO and $Co_{1-\delta}O$ are plotted versus ionic radius in fig. 5. The activation energy appears to vary systematically with the ionic radius if iron is a divalent ion in NiO and CoO in air. The ionic radius for Fe^{3+} is also shown in the figure. Iron ions in iron oxide in equilibrium in air are trivalent ions. Apparently the bonding in NiO and CoO lowers the energy of the crystal when the impurity is in the form of an Fe^{2+} ion rather than an Fe^{3+} ion.

Figure 5 also shows that the activation energy decreases when the ionic radius increases; the larger the ion, the more rapidly it diffuses! This unexpected feature occurs in nearly all tracer impurity studies in oxides considered in this review. The reason for this unanticipated behavior is not obvious. A detailed calculation of h_m^i, h_f^i, and C for a number of impurities in NiO or CoO is a reasonable problem for the HADES program; such a calculation could provide considerable understanding of this unusual experimental observation.

The observed values of ΔQ can be analyzed in terms of Δh_m, Δh_f and C for Co diffusion in NiO and to a lesser extent for Cr diffusion in NiO and $Co_{1-\delta}O$. First, we must establish values of Q^s, h_m^s, and h_f^s for NiO. The value of Q^s is rather well established; Atkinson and Taylor [20,21] and Volpe and Reddy [18] have measured cation self-diffusion in NiO over nearly seven orders of magnitude and obtain Q^s in the range 58 to 60 kcal/mol. We may take an average value of 59 kcal/mol. Three measurements of h_f^s provide a value of 19 kcal/mol [31-33]. The preferred experimental value of h_m^s is 37 kcal/mol [17]. Since the value of Q^s is probably the most reliable, and the value of h_m^s is probably the least reliable, we have adjusted the values of h_f^s and h_m^s (Table I) to satisfy the relation $Q^s = h_f^s + h_m^s$. Since both singly and doubly charged vacancies may contribute to diffusion in NiO, one may expect the effective activation enthalpies to vary slightly with temperature and p_{O_2}. However, the observed constant value of Q^s over seven orders of magnitude in D^* suggests that any temperature dependence of the effective activation enthalpies must be small in NiO.

The effect of impurity additions on impurity and self-diffusion in Co-doped NiO strongly suggests that the Co ion-vacancy binding energy must be small [23] (see section 5). The value of Q^i for Co tracer diffusion in NiO is 54 kcal/mol [23]. The temperature dependence of the isotope effect for ^{55}Co and ^{60}Co diffusion in NiO gives C = -4 kcal/mol and an analysis of C suggests that Δh_m is -10 kcal/mol [23] (see section 5). This leads to the defect parameters for Co impurity diffusion in NiO stated in Table I, which are also consistent with the defect parameters for pure NiO. This suggests that the impurity-vacancy binding energy may be small for homovalent impurities but the migration energy may be significantly different from that for self-diffusion.

Less extensive data exist for Cr tracer diffusion in NiO. The value of Q^i is 67 kcal/mol [24]; thus ΔQ = 8 kcal/mol. Since Cr ions diffuse much slower than Ni ions in pure NiO [fig. 3], w_2 must be much smaller than any other jump frequency, f^i must be nearly unity [see eq. (4)], and C must be close to zero. If chromium exists as Cr^{3+}, there should be an attractive interaction between Cr^{3+} and charged vacancies, i.e., Δh_f will be negative. This suggests that Δh_m must be greater than 8 kcal/mol and h_m^i must be greater than 47 kcal/mol. Values of the Cr interdiffusion coefficient in NiO at constant Cr concentration (i.e., constant vacancy concentration) suggest that $h_m^i - C - h_b^{i-V}$ is near 52 to 55 kcal/mol [34,35] (neglecting the temperature dependence of the thermodynamic factor). This suggests that h_m^i for Cr^{3+} diffusion in NiO may be even greater than 55 kcal/mol.

The value of Q^i is 58 kcal/mol for Cr tracer diffusion in CoO [30]; thus ΔQ = 20 kcal/mol. For the same reasons listed above for Cr diffusion in NiO, C must be close to zero and Δh_f should be negative for Cr diffusion in $Co_{1-\delta}O$. This suggests that Δh_m must be greater than 20 kcal/mol. Taking h_m^s = 32.6 kcal/mol [eq. (19)], one obtains h_m^i greater than 52 kcal/mol for Cr ions in $Co_{1-\delta}O$. This suggests that modest sized binding energies may be expected for trivalent impurities in a divalent matrix and the migration energy may be much larger than that for self-diffusion.

3. Impurity Diffusion in Fe_3O_4

3.1 Defect structure and cation self-diffusion in Fe_3O_4

Magnetite (Fe_3O_4) exists in the inverse spinel structure at low temperatures and is a metal-deficient oxide relative to the stoichiometric composition [36] at all but the lowest p_{O_2} for which the phase is stable [37,38]; the deviation from stoichiometry increases with increasing p_{O_2}. At low temperatures, one-eighth of the 64 cation tetrahedral sites and one-fourth of the 32 cation octahedral sites in the unit cell are occupied by Fe^{3+} ions while one-fourth of the octahedral sites are occupied by Fe^{2+} ions [39,40]. At higher temperatures electron interchange occurs, leading to a random distribution of the Fe^{2+} and Fe^{3+} ions among the occupied tetrahedral and octahedral sites [41].

Dieckmann and Schmalzried [42] recently reported measurements of D^*_{Fe} in Fe_3O_4 that show a minimum in the plot of log D^*_{Fe} versus log p_{O_2}, as seen in fig. 6. These results may be explained in terms of the following model

[38]: At low p_{O_2}, where Fe_3O_4 is stoichiometric, the intrinsic defects are Frenkel pairs; thus, iron diffusion is dominated by the more mobile iron interstitial ions. As p_{O_2} increases, and vacancies form on the iron sublattice [37], the iron interstitial ion concentration decreases, causing D^*_{Fe} to decrease. However, as p_{O_2} continues to increase, a point is reached beyond which the vacancy component completely dominates the diffusion process; from that point on, D^*_{Fe} increases with increasing p_{O_2}.

This model may be stated in terms of reactions involving vacancies on octahedral (V_O) or tetrahedral (V_T) sites and iron ions of two different charge states on interstitial sites (Fe_I^{3+}, Fe_I^{2+}). For sufficiently small point-defect concentrations, one obtains the relations

$$[V_O] \propto [V_T] \propto (p_{O_2})^{2/3} \tag{21}$$

and

$$[Fe_I^{2+}] \propto [Fe_I^{3+}] \propto (p_{O_2})^{-2/3} \ . \tag{22}$$

The results of Dieckmann and Schmalzried [42] (fig. 6) show a slope $\partial \log D^*_{Fe} / \partial \log p_{O_2} = -2/3$ at low p_{O_2}, as suggested by eq. (22) if the defect mobility is independent of p_{O_2}. At high p_{O_2} a slope near +2/3 is observed, as expected from eq. (21). A model with a random vacancy distribution between the tetrahedral and octahedral sites is entirely consistent with the data.

Peterson et al. [43] have recently measured D^*_{Fe} and the isotope effect for cation self-diffusion as a function of p_{O_2} at 1200°C in Fe_3O_4 in order

to differentiate between the free-interstitial mechanism and the interstitialcy mechanism at lower p_{O_2} and to verify the importance of the vacancy mechanism at higher p_{O_2}. The isotope-effect results at the higher p_{O_2} levels are entirely consistent with diffusion by the vacancy mechanism. The isotope effect at the lower p_{O_2} levels (interstitial region) is about half that at the higher levels. Since the correlation factor for diffusion by free interstitials is generally larger than for vacancies, the smaller value of the isotope effect at the two lower p_{O_2} values must arise principally from a two-atom jump process. Thus, the interstitial-type mechanism at lower p_{O_2} must be an interstitialcy mechanism.

Peterson et al. [43] evaluated the correlation factor for two types of vacancy jumps (tetrahedral and octahedral sublattice) and seven types of interstitialcy jumps in Fe_3O_4. Two different types of jumps involving the normally occupied tetrahedral sites are shown in fig. 7; the positions of the oxygen ions have been omitted from the figure for clarity. In mechanism (1), a vacancy can jump to any one of its four nearest-neighbor occupied sites. In mechanism (2), an interstitial ion at position 1 jumps into the normally occupied tetrahedral site at position 0 and the ion at position 0 jumps into interstitial site 2, 3 or 4. The interstitial sites in mechanism (2) are normally unoccupied octahedral sites. The jumps in mechanism (2) are "dog-leg" or noncollinear interstitialcy jumps involving the simultaneous motion of two atoms. (For a description of the vacancy

jumps on the octahedral sublattice and the other six types of interstitialcy jumps considered, as well as the calculation of the correlation factor for these jumps, see ref. 43.)

Both types of vacancy jumps are consistent with the isotope effect results with ΔK near unity, and five of the seven interstitialcy jumps are consistent with the isotope effect results. On the basis of the available space and location of atoms in the lattice, one might guess that unoccupied octahedral sites are the most likely interstitial sites for interstitialcy diffusion on both the tetrahedral and octahedral sublattice of Fe_3O_4. Under these conditions, the interstitialcy mechanism shown in fig. 7 is the most probable interstitial-type mechanism in Fe_3O_4.

3.2 Results for impurity diffusion in Fe_3O_4

Tracer impurity diffusion has been measured for ^{60}Co and ^{51}Cr in Fe_3O_4 [44]. The plots of log D^* vs log p_{O_2} show a minimum (see fig. 8), as observed for cation self-diffusion. The minimum occurs at nearly the same p_{O_2}, and $\partial \log D^*/\partial \log p_{O_2}$ is the same, for both impurity diffusion and self-diffusion [44]. This implies that the impurities diffuse by the same defect mechanism responsible for self-diffusion. This is easy to see for higher p_{O_2} where the vacancy mechanism is responsible for self-diffusion; only the vacancy concentration varies with p_{O_2}, so $\partial \log D^*/\partial \log p_{O_2}$ may be expected to be the same for both impurity and self-diffusion. For the same interstitial-type defect to be responsible for both impurity and self-diffusion, a two-atom process (i.e., an interstitialcy mechanism) must be

involved. Thus, the mechanism of diffusion required by the isotope effect measurements for self-diffusion is entirely consistent with the impurity-diffusion data for Fe_3O_4. This suggests that for those systems where $\partial \log D^*/\partial \log p_{O_2}$ for self-diffusion requires an interstitial-type mechanism, a similar measurement for impurity diffusion should yield an identical value of $\partial \log D^*/\partial \log p_{O_2}$ if an interstitialcy mechanism is operating but may yield a different value of the slope for impurity diffusion if an interstitial mechanism is responsible for self-diffusion.

As in the case of impurity diffusion in CoO and NiO, the smaller impurity Cr diffuses much slower (by a factor of 2 to 3 orders of magnitude) than the larger impurity Co. The similarity in the diffusion behavior of ^{60}Co and ^{59}Fe may suggest that tracer diffusion of Fe in Fe_3O_4 is governed primarily by the motion of Fe^{2+}. The slow migration of Cr may reflect the migration rate of Fe^{3+}. The high mobility of the electron holes allows any given Fe ion to change charge states many times between jumps. Thus the Fe ion will jump primarily when it is in the more mobile charge state (i.e., Fe^{2+}).

Dieckmann et al. [44] have also deduced an "apparent motion enthalpy," equal to $h_m^i - C - h_b^{i-v}$ in the present notation of eq. (5), for diffusion in the vacancy regime in Fe_3O_4. They obtain 32.9 kcal/mol for ^{59}Fe, 32.9 kcal/mol for ^{60}Co, and 58.8 kcal/mol for ^{51}Cr migration in Fe_3O_4.

4. Impurity Diffusion in TiO_2

4.1 Atomic and defect structure of TiO_2

The crystal structure of rutile (TiO_2) is noncubic and may be seen in fig. 9. The sublattice of the Ti^{4+} ions is body-centered tetragonal. The structure may be viewed as consisting of TiO_6 octahedra sharing edges and corners in such a way that each oxygen ion belongs to three neighboring octahedra. The oxygen octahedra are slightly distorted. When two unit cells are placed side by side and observed parallel to the c-axis, open channels become apparent, fig. 9b; open channels perpendicular to the c-axis are not apparent. The open channels will cause anisotropy in the diffusion process and may allow fast diffusion of smaller ions parallel to the c-axis.

The dominant defects in rutile are still under discussion even though numerous studies using a variety of techniques have been reported in the literature. Data supporting oxygen vacancies, V_O, or titanium interstitials, Ti_i, may be found. Kofstad [45] first proposed a defect model comprising both doubly charged oxygen vacancies and interstitial titanium ions with three and four effect charges. He suggests that $V_O^{\cdot\cdot}$ predominates at high oxygen partial pressures and low temperatures whereas Ti_i^{3+} and Ti_i^{4+} are suggested as dominant defects at higher temperatures and lower oxygen pressure. Recent conductivity and thermogravimetry measurements by Marucco [46] further support this model, and suggest the additional possibility that singly charged oxygen vacancies $V_O^{\cdot}$ become important at the highest

p_{O_2}. Both cation tracer diffusion [47] and proton channeling [48] experiments demonstrate that the predominant defect of the metal sublattice is the titanium interstitial.

4.2 Impurity diffusion in TiO_2

As noted above, open channels exist parallel to the c-axis in TiO_2, and may allow fast diffusion of small impurity ions. Making certain assumptions about the degree of ionicity of the Ti-O bond and using Pauling's ionic and covalent radii for Ti and O, Wittke [49] estimates the interstitial diffusion channels to consist of chains of "voids" of approximately 0.77 Å radius, joined by deformed regions of comparable cross-sectional area.

Johnson [50] was the first to measure the migration of a small ion, Li^+ (r_i = 0.62 Å), in TiO_2. He observed that lithium diffusion parallel to the c-axis (along the direction of the open channels) is at least 10^8 times faster than perpendicular to the c-axis. A good Arrhenius plot was observed for $D_{\parallel c}$ with $D_o \sim 0.3$ cm^2/sec and $Q_{\parallel c}$ = 7.6 kcal/mol. This gives $D^{Li}_{\parallel c} \sim 10^{-3}$ cm^2/sec at T ~ 500°C compared to an extrapolated value of $D^{Ti}_{\parallel c} \sim 10^{-18}$ cm^2/sec at a similar temperature. Although an indirect method (optical absorption) was used to determine D^{Li} and Li was present in bulk quantities (hence, diffusion in a chemical gradient was measured), the large value of $D^{Li}_{\parallel c}$, the small value of $Q_{\parallel c}$, and the large anisotropy are strong support for the channel model and interstitial diffusion. The channel mechanism presumably works best in an ideal crystal (unlike most

diffusion mechanisms). Johnson [50] has observed that Li diffusion in TiO_2 was strongly influenced by abrasion of the surface. Since dislocations or stacking faults introduced by grinding may close off channels, these observations further support the channel model of diffusion.

Another small interstitial impurity atom, H, also shows rapid diffusion ($D^H_{\parallel c} \sim 3\times10^{-7}$ cm^2/sec at T = 500^{0}C) and considerable anisotropy in the diffusion coefficients [51] ($D^H_{\parallel c}/D^H_{\perp c} \sim 150$ at T = 500^{0}C) in TiO_2. However, owing to the interaction of the H^+ with oxygen ions, the mechanism of migration of H^+ may be more complicated and involve the formation, rotation, and dissociation of OH [52].

Wittke [49] has made qualitative observations of color change in TiO_2 crystals which suggest that Cr, Fe, Co, and Ni diffuse rapidly along the c-axis. Similar qualitative observations have been reported by Steele and McCartney [53] which support the conclusion that $D^{Fe}_{\parallel c} > D^{Fe}_{\perp c}$ in TiO_2. One may expect Cr^{3+} (0.62 Å), Fe^{3+} (0.65 Å), Co^{2+} (0.74 Å), and Ni^{2+} (0.69 Å) to diffuse rapidly through the 0.77 Å channels, in contrast to oxygen or larger impurities.

Sasaki and Peterson [54] have made preliminary tracer diffusion studies of ^{60}Co and ^{51}Cr in TiO_2, both parallel and perpendicular to the c-axis. They observe that $D^{Co}_{\parallel c}$ is about 10^7 times greater than $D^{Ti}_{\parallel c}$ (at 800°C) with D_o = 3.9 cm^2/sec and Q = 33 kcal/mol. The value of $D^{Co}_{\perp c}$ is not as well established but $D^{Co}_{\parallel c}/D^{Co}_{\perp c}$ is at least 10^3. Chromium diffusion in TiO_2 [54], like cation self-diffusion [55], shows relatively little anisotropy. However, even though Cr^{3+} is nearly 20% smaller than Co^{2+}, $D^{Co}_{\parallel c} \approx 10^5\, D^{Cr}_{\parallel c}$ in

TiO_2. It is clear that ionic size alone is not a good criterion for rapid diffusion along the open channels in TiO_2. More extensive tracer impurity diffusion studies and state-of-the-art calculations will be needed before the effects of ionic size and charge on rapid diffusion in the open channels of TiO_2 are understood.

5. Effect of Impurities on Diffusion

5.1 Cobalt impurity diffusion in NiO

The presence of an impurity atom in an otherwise pure crystal will change the jump frequencies of the neighboring solvent atom relative to the values in the absence of the impurity. The correlation factor for impurity diffusion f^i must be stated in terms of a number of different jump frequencies, as shown in eq. (4) (fig. 1). For each impurity atom added to the solvent, a known number of solvent atoms will jump with a frequency w_1, w_3, or w_4 rather than w_o. Lidiard [56] was the first to derive the average solvent-atom jump frequency as a function of impurity content c in terms of the various w_i's. He found that the self-diffusion coefficient in an alloy of composition c, $D^S(c)$, could be written as

$$D^S(c) = D^S(o)(1 + bc), \tag{23}$$

where $D^S(o)$ is the solvent ion diffusion coefficient in the pure solvent. The enhancement factor b is expressed by

$$b = -18 + 4\left[\frac{w_1}{w_o} + \frac{7}{2}\frac{w_3}{w_o}\right] \exp(h_b^{i-v}/kT) \tag{24}$$

within the framework of the Lidiard theory. Here, the impurity vacancy binding energy h_b^{i-v} may be expressed in terms of the jump frequency ratio

$$w_4/w_3 = \exp(h_b^{i-v}/kT). \tag{25}$$

The ratio of the impurity diffusion coefficient $D^i(o)$ to the solvent diffusion coefficient in the otherwise pure solvent is given by [56]

$$\frac{D^i(o)}{D^s(o)} = \frac{f^i}{f^s}\frac{w_2}{w_o}\exp(h_b^{i-v}/kT), \tag{26}$$

where f^s is the correlation factor for solvent self-diffusion. Thus, from the experimentally measured quantities f^i, b, and $D^i(o)/D^s(o)$, one obtains information about the various jump processes near an impurity ion.

In deriving eq. (24), Lidiard assumed that all solvent jumps in the alloy have a correlation factor f^s as in the pure solvent. Howard and Manning [57] have removed this assumption and found that, for a given set of values of $D^i(o)$, $D^s(o)$, and b, a range of possible values of f^i exist, and that unique values of w_4/w_o, w_3/w_1, and w_2/w_1 correspond to each value of f^i. Hence, given experimental values of $D^i(o)$, $L^s(o)$, b, and f^i, a unique set of jump-frequency ratios may be obtained. Experiments of this type have been performed for impurity diffusion in metals [58-60]; however, for the following discussions, Lidiard's theory will be sufficient.

In an attempt to study the detailed process of cation impurity diffusion and the effect of impurity-defect interactions on cation self-diffusion in oxides, Chen and Peterson [23] have measured the isotope effect for cobalt diffusion in NiO and the dependence of cobalt and nickel

diffusivities on dilute cobalt concentrations in $(Ni_{1-c}Co_c)O$ crystals. The experimental values of $(f\Delta K)_{Co}$, deduced from measurements of the simultaneous diffusion of ^{55}Co and ^{60}Co in NiO, increase from 0.45 ± 0.01 at 1179°C to 0.61 ± 0.01 at 1649°C. The correlation factor f_{Co} was determined from the product $(f\Delta K)_{Co}$ by assuming that ΔK for cobalt impurity diffusion is the same as that for nickel self-diffusion in NiO ($\Delta K = 0.78$), and f_{Co} is plotted as a function of temperature in fig. 10. The slope of the line in fig. 10 gives C = -4 kcal/mol, a value used in Section 2.3 and Table I.

The diffusion coefficients for both cobalt and nickel diffusion in $(Ni_{1-c}Co_c)O$ crystals increase linearly with cobalt concentrations (up to c = 0.015) at precisely the same rate. The equal enhancement for both solvent and solute diffusion is further demonstrated by the fact that the ratios of D_{Co}/D_{Ni}, obtained from the simultaneous diffusion of ^{60}Co and ^{57}Ni, are independent of composition at a given temperature.

Lidiard's theory has successfully explained the effect of solute additions on self-diffusion in many metallic systems; however, it does not predict the enhancement of solute diffusivity. By extending Lidiard's analysis, one can show that the association of a vacancy with two solute atoms may result in a linear enhancement for solute diffusion, and will add a quadratic term to the expression for the enhancement of the solvent diffusivity [3]. Thus both solvent and solute diffusion may be enhanced by additions of solute, but the enhancement effect for solvent diffusion

should be greater than that for solute diffusion. This prediction is contrary to the experimental results for the $(Ni_{1-c}Co_c)O$ crystals.

In addition to the effects of solute additions on self-diffusion considered by Lidiard for metallic systems, an effect in oxide systems arises from charge neutrality conditions. Since the third ionization energy for Co^{3+} is lower than that for Ni^{3+}, the concentration of cation vacancies must vary at a given temperature in a dilute oxide solid solution to conserve charge neutrality. This will cause the free-vacancy concentration to vary linearly with cation composition. The combined effect of the vacancy-solute interactions given by Lidiard and the change in free-vacancy concentration result in the enhancement factors $b_1 = b + b_V$ and $B_1 = b_V$ for the diffusion of solvent and solute, respectively. Here b_V is the contribution to the enhancement of diffusivity due to increased free-vacancy concentration. Since the experimental results show that $b_1 = B_1$ and D^i/D^s are constant values independent of Co concentration at a given temperature, the enhancement of both cobalt and nickel diffusion is primarily caused by the increased concentration of cation vacancies; the vacancy-solute interactions and their contribution to the enhancement of solvent diffusion are negligible ($b \approx 0$).

These conclusions suggest that $h_b^{i-v} \ll kT$ and $w_o = w_1 = w_3 = w_4 \neq w_2$. Using these conditions, w_2/w_o and D_{Co}/D_{Ni} in pure NiO were calculated as a function of temperature from only the measured values of f_{Co} using eqs. (4) and (26). The calculated values of w_2/w_o and D_{Co}/D_{Ni} are plotted versus temperature in fig. 11. The temperature dependence of w_2/w_o gives directly

References

[1] A. D. LeClaire, in: Physical chemistry, Vol. 10, eds. H. Eyring, D. Henderson and W. Jost (Academic Press, N.Y.), Chapter 5.

[2] J. R. Manning, Phys. Rev. 136 (1964) A1758.

[3] A. D. LeClaire, J. Nucl. Mat. 69&70 (1978) 70.

[4] P. Kofstad, in: Nonstoichiometry, diffusion, and electrical conductivity in binary metal oxides (J. Wiley & Sons, New York, 1972).

[5] R. E. Carter and F. D. Richardson, Trans. AIME 200 (1954) 1244.

[6] P. Fisher and D. S. Tannhauser, J. Chem. Phys. 44 (1966) 1663.

[7] H.-G. Sockel and H. Schmalzried, Ber. Bunsenges. Phys. Chem. 72 (1968) 745.

[8] N. G. Eror and J. B. Wagner, Jr., J. Phys. Chem. Solids 29 (1968) 1597.

[9] I. Bransky and J. M. Wimmer, J. Phys. Chem. Solids 33 (1972) 801.

[10] E. Fryt, Oxid. Met. 10 (1976) 311.

[11] W. K. Chen. N. L. Peterson and W. T. Reeves, Phys. Rev. 186 (1969) 887.

[12] W. F. Crow, Ph.D. Thesis, Ohio State University (1969).

[13] R. Dieckmann, Z. Phys. Chem. Neue Folge 107 (1977) 189.

[14] W. K. Chen and N. L. Peterson, J. Phys. Chem. Solids 41 (1980) 647.

[15] W. K. Chen and R. A. Jackson, J. Phys. Chem. Solids 30 (1969) 1309.

[16] M. Gvishi and D. S. Tannhauser, J. Phys. Chem. Solids 33 (1972) 893.

[17] R. Farhi and G. Petot-Frvas, J. Phys. Chem. Solids 39 (1978) 1169; ibid. 39 (1978) 1175.

[18] M. L. Volpe and J. Reddy, J. Chem. Phys. 53 (1970) 1117.

[19] N. L. Peterson and W. K. Chen, J. Phys. Chem. Solids 43 (1982) 29.

[20] A. Atkinson and R. I. Taylor, J. Mater. Sci. 13 (1978) 427.

[21] A. Atkinson and R. I. Taylor, Phil. Mag. A 39 (1979) 581.

[22] W. K. Chen and N. L. Peterson, J. Phys. Chem. Solids 34 (1973) 1093.

[23] W. K. Chen and N. L. Peterson, J. Phys. Chem. Solids 33 (1972) 881.

[24] W. K. Chen, N. L. Peterson and L. C. Robinson, J. Phys. Chem. Solids 34 (1973) 705.

[25] C. Dubois, Ph.D. Thesis, University of Paris (1979).

[26] D. R. Chang, R. Nemoto, and J. B. Wagner, Jr., Met. Trans. 7A (1976) 803.

[27] W.-Y. Howng and J. B. Wagner, Jr., J. Phys. Chem. Solids 39 (1978) 1019.

[28] P. Dumas, A. Fauvre, and J. C. Colson, Ann. Chim. (Paris) 4 (1979) 269.

[29] J. Sasaki and N. L. Peterson, unpublished results (1982).

[30] W. K. Chen, unpublished results (1982), and W. K. Chen, N. L. Peterson and G. J. Talaber, Bull. Am. Ceram. Soc. 60 (1981) 375.

[31] C. M. Osburn and R. W. Vest, J. Phys. Chem. Solids 32 (1971) 1331.

[32] Y. D. Tretyakov and R. A. Rapp, Trans. AIME 245 (1969) 1235.

[33] W. C. Tripp and N. M. Tallan, J. Am. Ceram. Soc. 53 (1970) 531.

[34] C. Greskovick, J. Am. Ceram. Soc. 53 (1970) 498.

[35] R. A. Perkins, Ph.D. Thesis, Ohio State University (1971).

[36] L. S. Darken and R. W. Gurry, J. Am. Ceram. Soc. 68 (1946) 798.

[37] H. G. Sockel and H. Schmalzried, Ber. Bunsenges. Phys. Chem. 72 (1968) 745.

[38] R. Dieckmann and H. Schmalzried, Ber. Bunsenges. Phys. Chem. 81 (1977) 414.

[39] E. J. W. Verwey, P. W. Honyman and F. C. Romeijn, J. Chem. Phys. 15 (1947) 181.

[40] C. P. Shull, E. O. Wollman and W. C. Koehler, Phys. Rev. 84 (1951) 912.

[41] C. C. Wu and T. O. Mason, J. Am. Ceram. Soc. 64 (1981) 520.

[42] R. Dieckmann and H. Schmalzried, Ber. Bunsenges. Phys. Chem. 81 (1977) 344.

[43] N. L. Peterson, W. K. Chen and D. Wolf, J. Phys. Chem. Solids 41 (1980) 709.

[44] R. Dieckmann, T. O. Mason, J. D. Hodge, and H. Schmalzried, Ber. Bunsenges. Phys. Chem. 82 (1978) 778.

[45] P. Kofstad, J. Less-Common Metals 13 (1967) 635.

[46] J.-F. Marucco, J. Gautron and P. Lemasson, J. Phys. Chem. Solids 42 (1981) 363.

[47] J. R. Akse and H. R. Whitehurst, J. Phys. Chem. Solids 39 (1978) 457.

[48] E. Yagi, A. Koyama, H. Sakairi and R. Hasiguti, J. Phys. Soc. Japan 42 (1977) 939.

[49] J. P. Wittke, J. Electrochem. Soc. 113 (1966) 193.

[50] O. W. Johnson, Phys. Rev. 136 (1964) A284.

[51] O. W. Johnson, S.-H. Paek and J. W. DeFord, J. Appl. Phys. 46 (1975) 1026.

[52] J. B. Bates, J. C. Wang and R. A. Perkins, Phys. Rev. B19 (1979) 4130.

[53] J. L. Steele and E. R. McCartney, Nature 222 (1969) 79.

[54] J. Sasaki and N. L. Peterson, work in progress, 1982.

[55] T. S. Lundy and W. A. Coghlan, J. Phys. Paris 34 (1973) C9-299.

[56] A. B. Lidiard, Phil. Mag. 5 (1960) 1171.

[57] R. E. Howard and J. R. Manning, Phys. Rev. 154 (1967) 561.

[58] S. J. Rothman and N. L. Peterson, Phys. Rev. 154 (1967) 552.

[59] N. L. Peterson and S. J. Rothman, Phys. Rev. 154 (1967) 558.

[60] N. L. Peterson and S. J. Rothman, Phys. Rev. B2 (1970) 1540.

Table I. Probable values of defect parameters in NiO (all values in kcal/mol).

(a) Self-Diffusion

O^s	h_f^s	h_m^s
59	20	39

(b) Impurity Diffusion

Impurity	O^i	h_f^i	h_b^{i-v}	h_m^i	C
Co	54	21	~ 0	29	-4
Cr	67	< 20	> 0	> 47	0

Figure Captions

Fig. 1. Vacancy jumps near an impurity in an fcc crystal.

Fig. 2. Cation self-diffusion as a function of the oxygen partial pressure in $Co_{1-\delta}O$ in the temperature range 1000-1400°C. From Dieckmann [13].

Fig. 3. Tracer diffusion in NiO at p_{O_2} = 0.21 atm. The data are from the following references: ^{55}Fe--Crow [12]; ^{60}Co--Chen and Peterson [22,23]; high-temperature ^{63}Ni--Volpe and Reddy [18] and Chen and Peterson [22]; low-temperature ^{63}Ni--Atkinson and Taylor [20,21]; ^{51}Cr--Chen, Peterson and Robinson [24]; ^{18}O--Dubois [25].

Fig. 4. Tracer diffusion in $Co_{1-\delta}O$ at p_{O_2} = 0.21 atm. The data are from the following references: ^{60}Co--Carter and Richardson [5], Chen, Peterson and Reeves [11], Chen and Peterson [22], and Dieckmann [13]; ^{55}Fe--Crow [12]; ^{57}Ni--Chen and Peterson [22]; ^{51}Cr--Chen [30]; ^{18}O--Chen and Jackson [15].

Fig. 5. Activation energy for tracer diffusion in NiO and $Co_{1-\delta}O$ vs ionic radius of the tracer ion.

Fig. 6. The cation self-diffusion coefficient in Fe_3O_4 as a function of p_{O_2} in the temperature range 900-1400°C. From Dieckmann and Schmalzried [42].

Fig. 7. Vacancy and interstitialcy jumps mainly involving cation tetrahedral sites in the Fe_3O_4 lattice. The oxygen sites are omitted for clarity. From Peterson et al. [43].

Fig. 8. Tracer diffusion in Fe_3O_4 as a function of the oxygen partial pressure at 1200-1210°C. The data are from the following references; ^{59}Fe--Dieckmann and Schmalzried [42]; ^{60}Co and ^{51}Cr--Dieckmann, Mason, Hodge, and Schmalzried [44].

Fig. 9. (a) A unit cell of the rutile (TiO_2) structure. (b) An end view of the atomic arrangement for the [001] axial direction. The open channel along the c-axis is indicated by the dashed lines.

Fig. 10. Log f_{Co} vs reciprocal absolute temperature for cobalt diffusion in NiO. From Chen and Peterson [23].

Fig. 11. Temperature dependence of (a) D_{Co}/D_{Ni} (●) and (b) w_2/w_o (▲) as calculated from measured values of f_{Co}. Experimental data from the simultaneous diffusion of ^{60}Co and ^{57}Ni (⊡) are also shown. From Chen and Peterson [23].

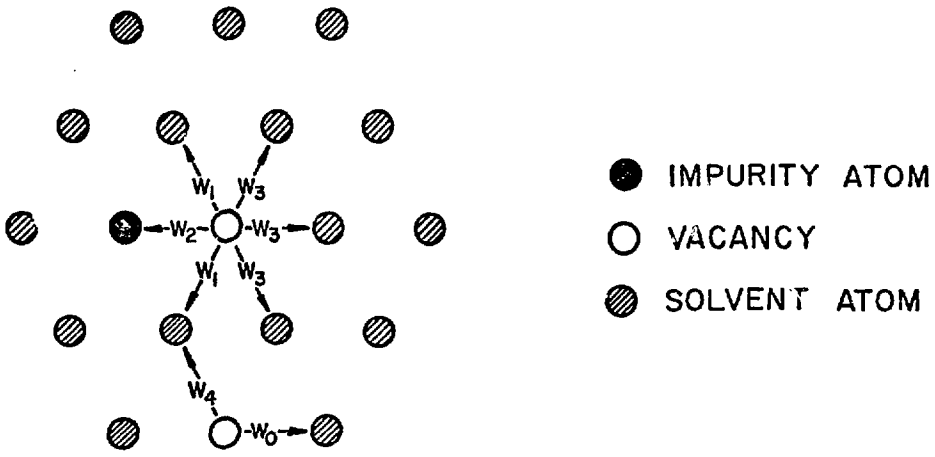

Fig. 1. Vacancy jumps near an impurity in an fcc crystal.

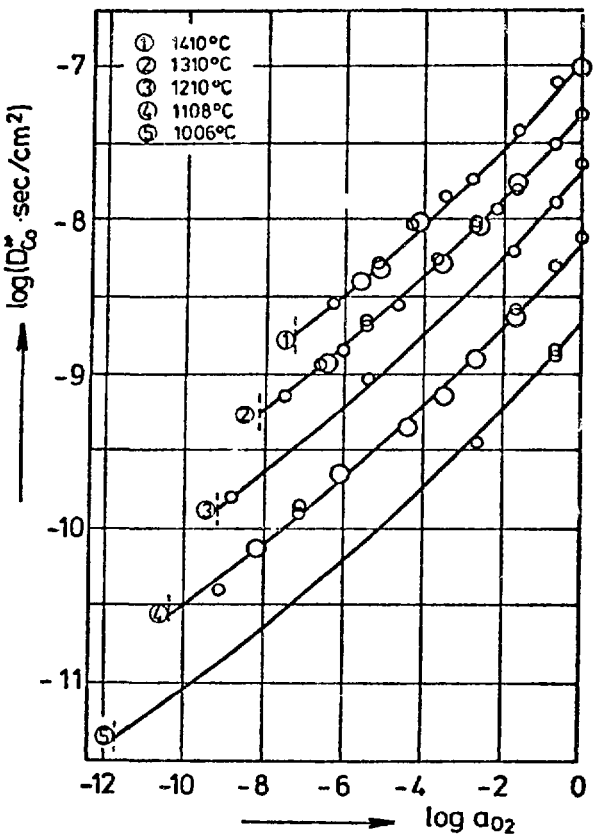

Fig. 2. Cation self-diffusion as a function of the oxygen partial pressure in $Co_{1-\delta}O$ in the temperature range 1000-1400°C. From Dieckmann [13].

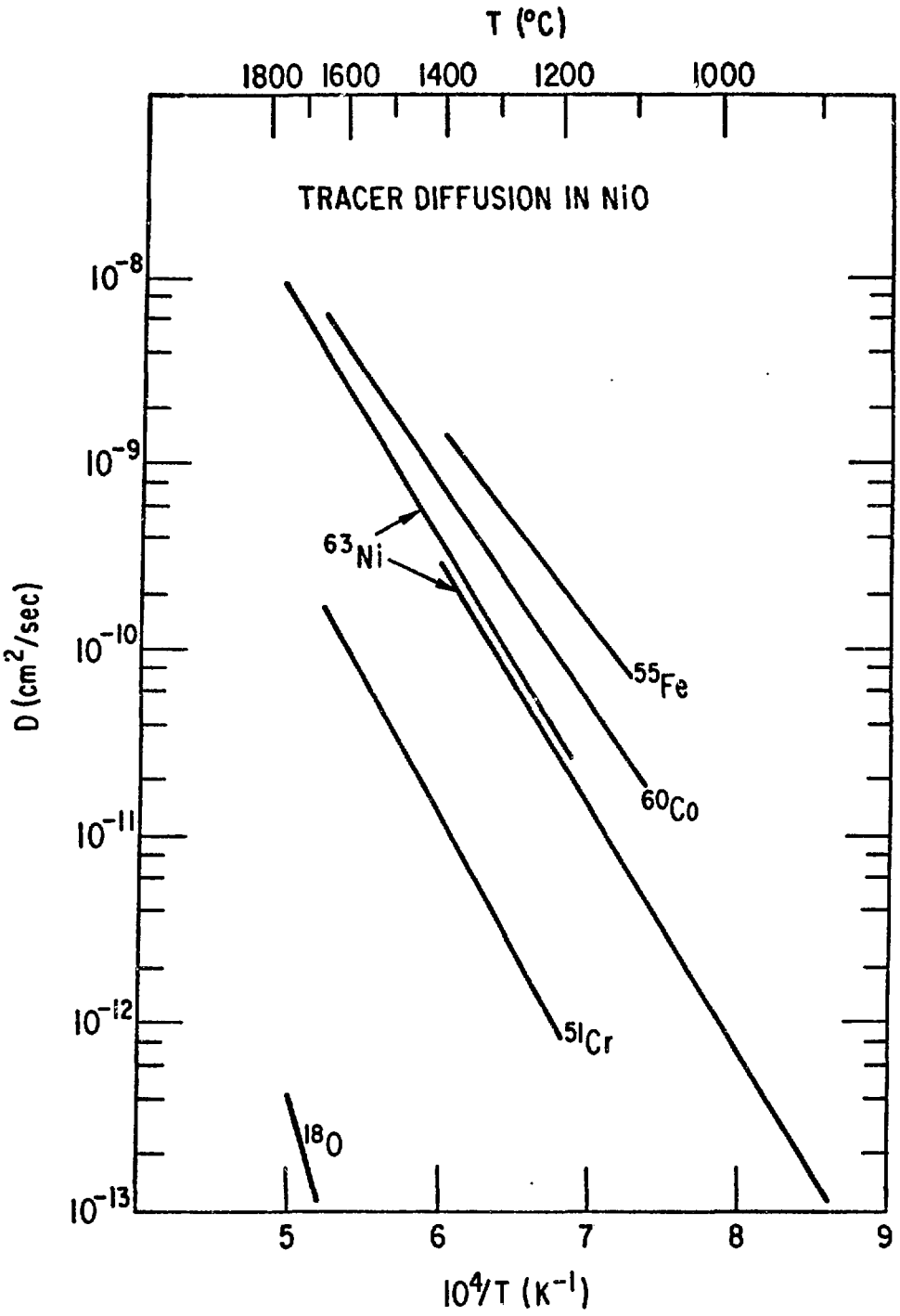

Fig. 3. Tracer diffusion in NiO at p_{O_2} = 0.21 atm. The data are from the following references: ^{55}Fe--Crow [12]; ^{60}Co--Chen and Peterson [22,23]; high-temperature ^{63}Ni--Volpe and Reddy [18] and Chen and Peterson [22]; low-temperature ^{63}Ni--Atkinson and Taylor [20,21]; ^{51}Cr--Chen, Peterson and Robinson [24]; ^{18}O--Dubois [25].

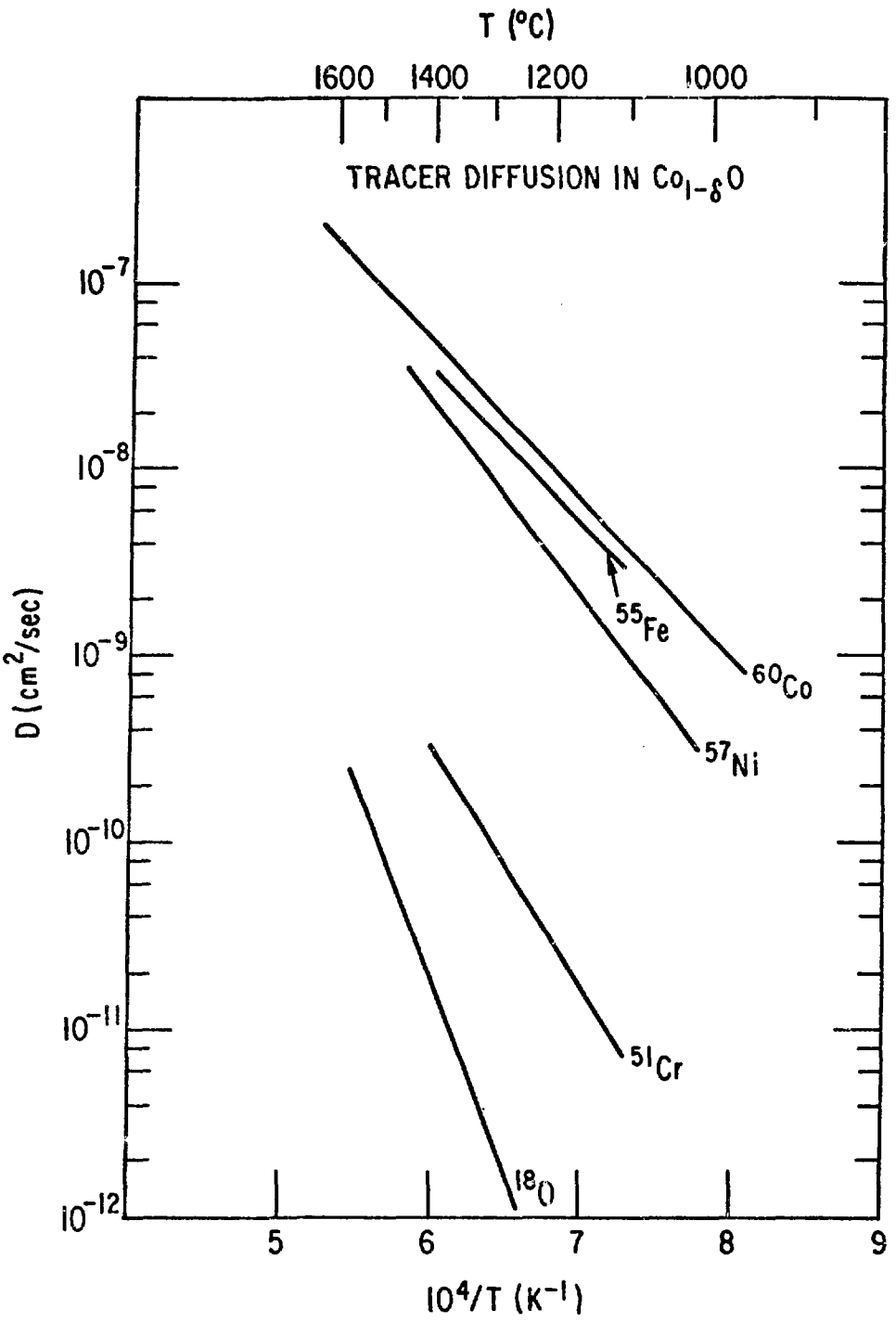

Fig. 4. Tracer diffusion in $Co_{1-\delta}O$ at p_{O_2} = 0.21 atm. The data are from the following references: ^{60}Co--Carter and Richardson [5], Chen, Peterson and Reeves [11], Chen and Peterson [22], and Dieckmann [13]; ^{55}Fe--Crow [12]; ^{57}Ni--Chen and Peterson [22]; ^{51}Cr--Chen [30]; ^{18}O--Chen and Jackson [15].

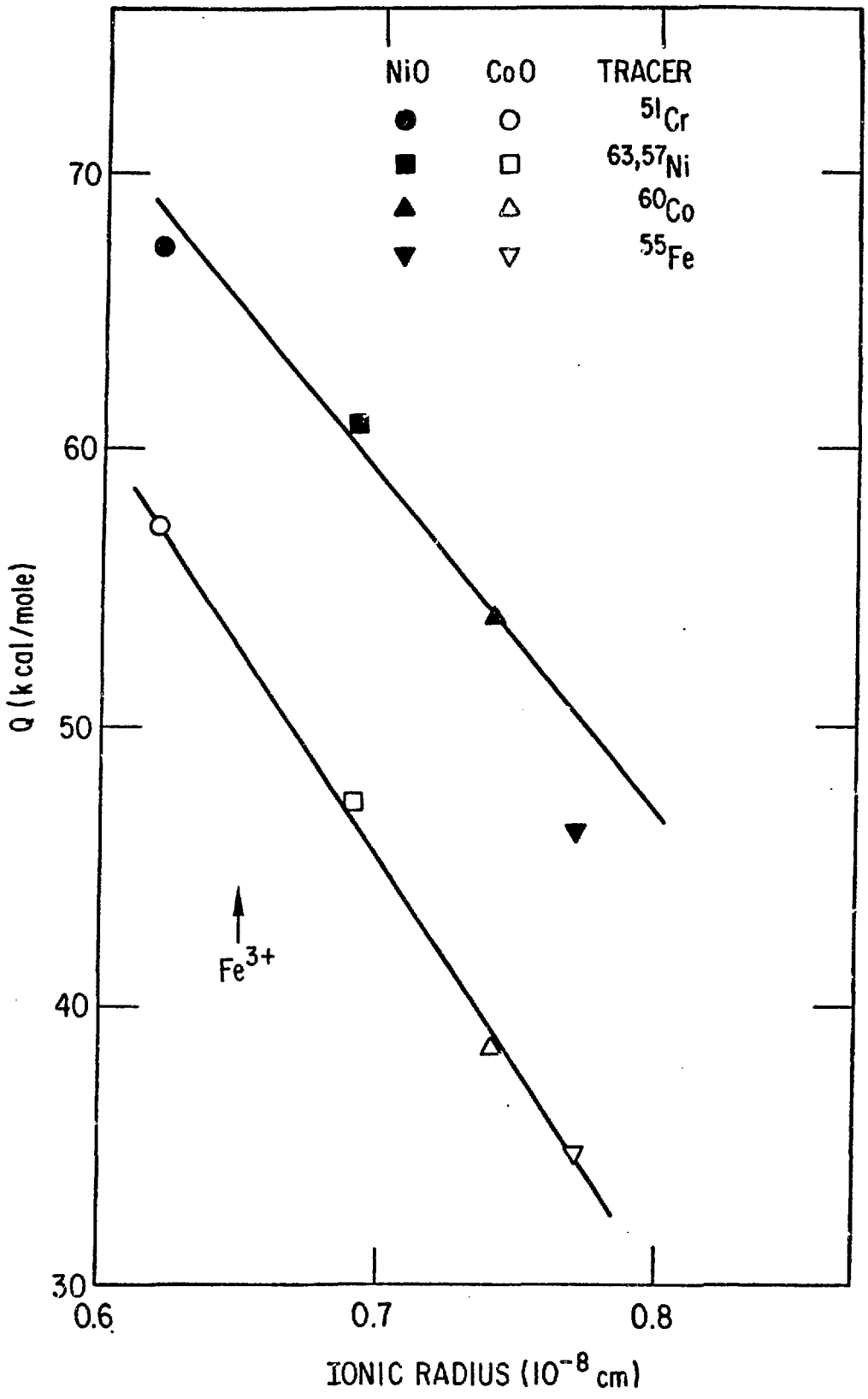

Fig. 5. Activation energy for tracer diffusion in NiO and $Co_{1-\delta}O$ vs ionic radius of the tracer ion.

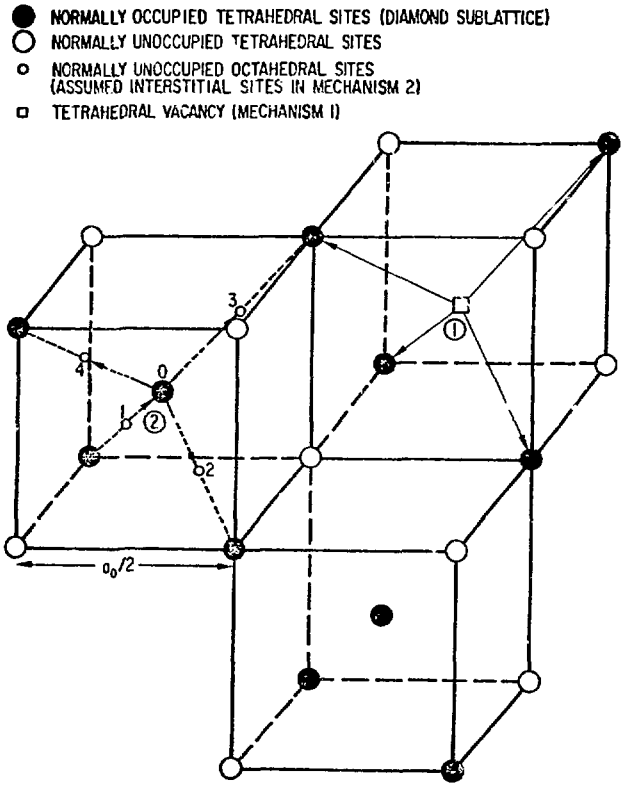

Fig. 7. Vacancy and interstitialcy jumps mainly involving cation tetrahedral sites in the Fe_3O_4 lattice. The oxygen sites are omitted for clarity. From Peterson et al. [43].

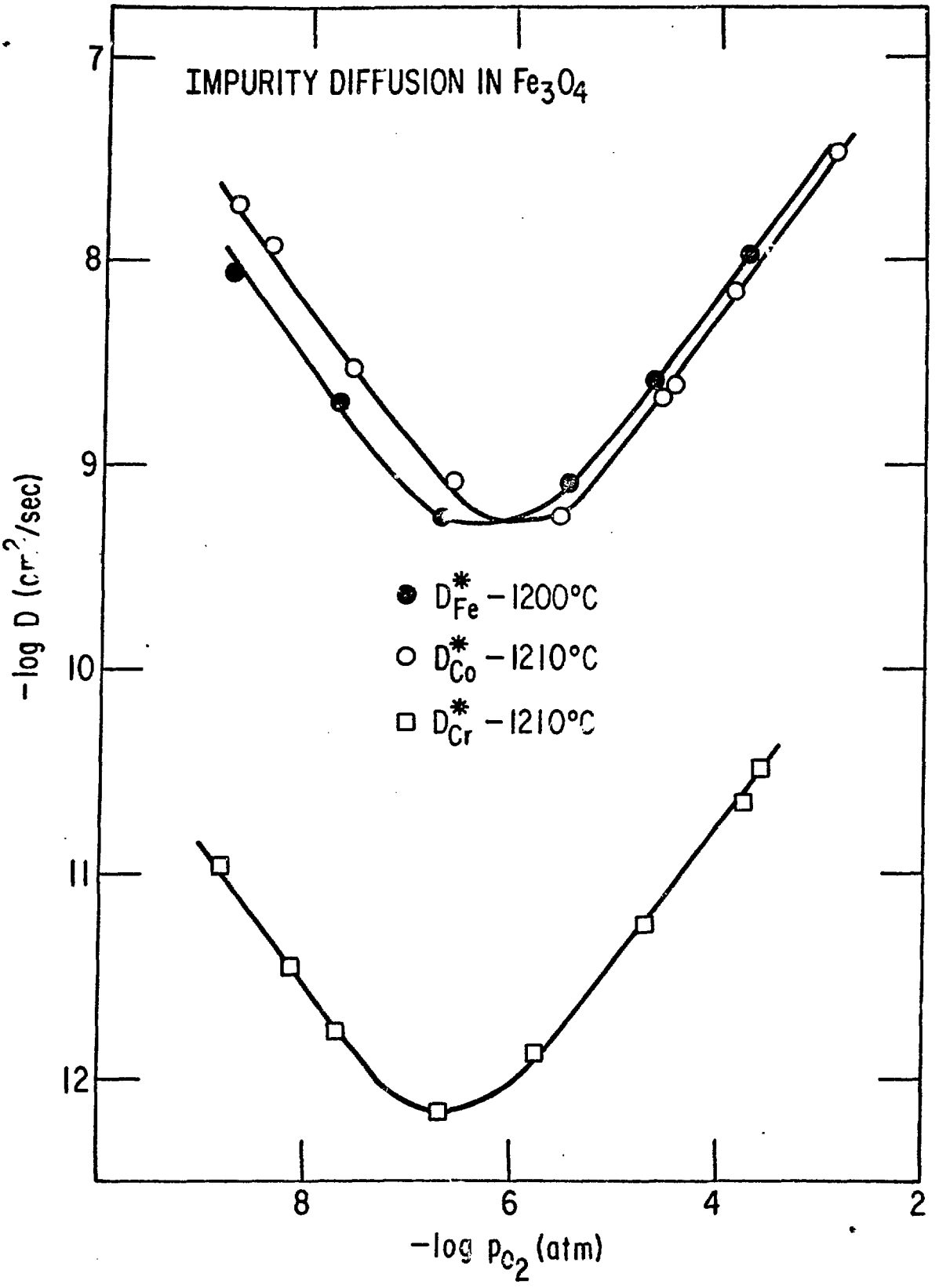

Fig. 8. Tracer diffusion in Fe_3O_4 as a function of the oxygen partial pressure at 1200-1210°C. The data are from the following references; ^{59}Fe--Dieckmann and Schmalzried [42]; ^{60}Co and ^{51}Cr--Dieckmann, Mason, Hodge, and Schmalzried [44].

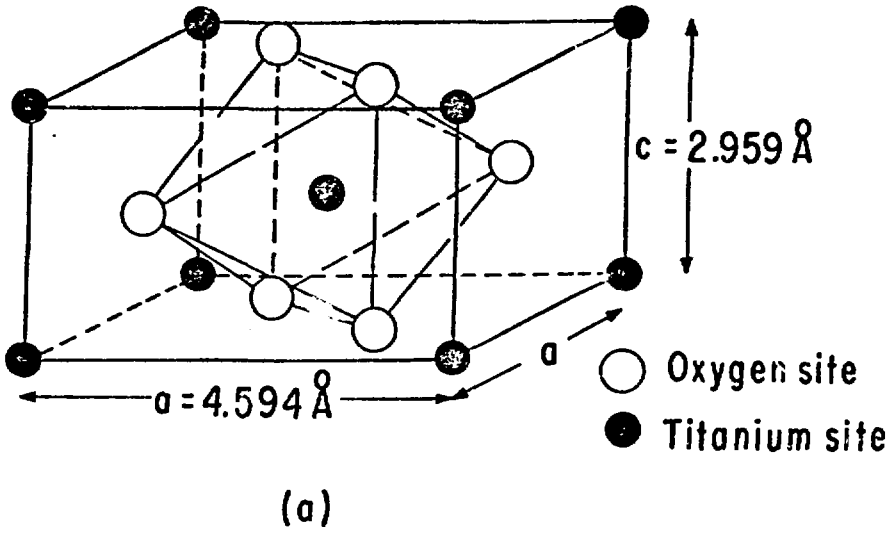

(a)

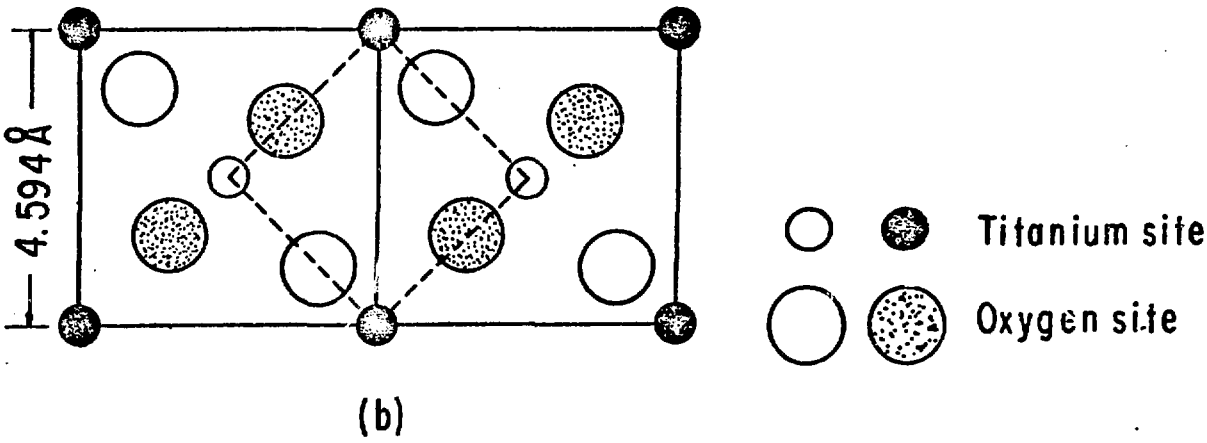

(b)

Fig. 9. (a) A unit cell of the rutile (TiO_2) structure. (b) An end view of the atomic arrangement for the [001] axial direction. The open channel along the c-axis is indicated by the dashed lines.

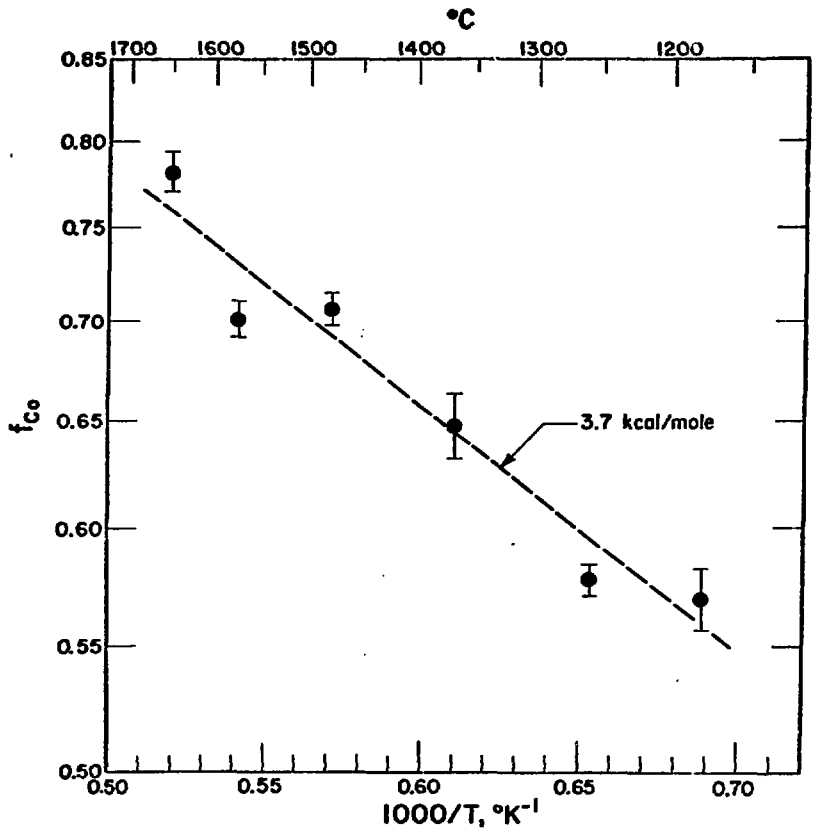

Fig. 10. Log f_{Co} vs reciprocal absolute temperature for cobalt diffusion in NiO. From Chen and Peterson [23].

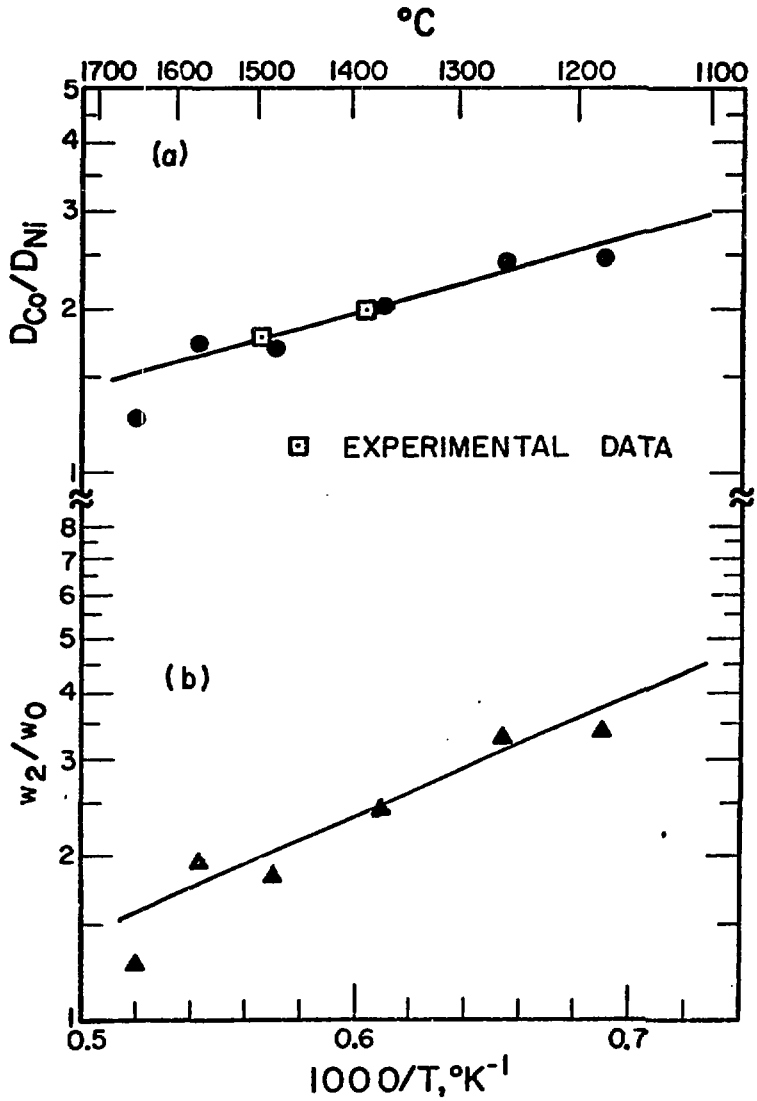

Fig. 11. Temperature dependence of (a) D_{Co}/D_{Ni} (●) and (b) w_2/w_o (▲) as calculated from measured values of f_{Co}. Experimental data from the simultaneous diffusion of ^{60}Co and ^{57}Ni (⊡) are also shown. From Chen and Peterson [23].